Free Fatty Acid Uptake in the Myocardium and Skeletal Muscle Using Fluorine-18-Fluoro-6-Thia-Heptadecanoic Acid

Maija T. Mäki, Merja Haaparanta, Pirjo Nuutila, Vesa Oikonen, Matti Luotolahti, Olli Eskola and Juhani M. Knuuti
Departments of Nuclear Medicine, Medicine and Clinical Physiology, and Radiochemistry Laboratory, University of Turku, Turku; and Turku PET Centre, Turku, Finland

14(R,S)-[^{18}F]fluoro-6-thia-heptadecanoic acid (FTHA) has been recently introduced as a new tracer for fatty acid metabolism. Myocardial [^{18}F]FTHA uptake is believed to reflect mainly beta-oxidation of the circulating free fatty acids (FFAs), since it is trapped in the mitochondria because subsequent steps of beta-oxidation are inhibited by sulfur heteroatom. We investigated [^{18}F]FTHA kinetics in myocardial and skeletal muscle in vivo. **Methods:** Two dynamic PET studies were performed in seven patients with stable coronary artery disease, once in the fasting state and once during euglycemic hyperinsulinemia (serum insulin ~60 mU/liter). The fractional [^{18}F]FTHA uptake rates (K_i) were multiplied with serum FFA concentrations and were considered to represent FFA uptake. **Results:** Serum FFA concentration decreased by 80% during insulin clamp. After tracer injection, rapid myocardial uptake was identified both in the fasting state and during insulin stimulation. The cardiac image quality was excellent in both occasions. In addition, femoral muscles were clearly visualized in both studies. The fractional myocardial [^{18}F]FTHA uptake rates (K_i) in the normal myocardial regions were similar in the fasting state (0.11 ± 0.04 ml/g/min (mean ± s.d.) and during insulin clamp (0.12 ± 0.03 ml/g/min; ns). The calculated myocardial FFA uptake was four times higher in the fasting state than during insulin clamp (5.8 ± 1.7 versus 1.4 ± 0.5 μmol/100 g/min, $p < 0.005$). The femoral muscle fractional [^{18}F]FTHA uptake rates (K_i) were lower (0.0071 ± 0.0014 ml/g/min) in the fasting state than during insulin clamp (0.0127 ± 0.0036 ml/g/min; $p = 0.03$), but the estimated femoral muscle FFA uptake was three times higher in the fasting state (0.38 ± 0.09 μmol/100 g/min) as compared to that during insulin clamp (0.12 ± 0.05 μmol/100 g/min, $p < 0.005$). **Conclusion:** Fluorine-18-FTHA PET appears to be a feasible method to estimate fatty acid kinetics in myocardial and skeletal muscle. Physiologically reasonable rates of FFA uptake in myocardium and skeletal muscle were obtained. Furthermore, the uptake rates were suppressed in response to insulin both in the myocardial and femoral muscle as expected.

Key Words: free fatty acids; fluorine-18-fluoro-6-thia-heptadecanoic acid; muscle; myocardium; PET

J Nucl Med 1998; 39:1320–1327

Free fatty acids (FFAs) are the primary source of energy in the well-oxygenated myocardium (*1–3*) and skeletal muscle (*4–6*) in the fasting state. Rate of FFA utilization by cardiac muscle is determined by the availability of exogenous fatty acids and the rate of oxidative metabolism or workload of the heart (*1,3,7*). Insulin lowers plasma FFA levels by inhibiting lipolysis in adipose tissue (*8*). When plasma glucose and insulin levels are increased, the myocardium preferentially uses glucose while fatty acid uptake and oxidation are suppressed (*9–11*). Insulin lowers FFA uptake (*5,12*) and oxidation (*5*) also in the limb. In experimental studies, the FFA beta-oxidation has been impaired during myocardial ischemia (*1,13*), even before the changes in cardiac function or electrocardiogram appear. The alterations of fatty acid metabolism has not been fully investigated in many other conditions and diseases such as diabetes or hypertension. Therefore, a technique that allows study of local FFA metabolism in humans would be important.

Fatty acids or fatty acid analogs labeled with radioactive isotopes have been used for noninvasive delineation of myocardial metabolism (*7*). The radioiodinated long-chain fatty acids can be traced with conventional gamma cameras but they lack the possibility of quantification. PET allows us to evaluate noninvasively and quantitatively changes in myocardial metabolism. However, distribution of FFAs into various lipid pools and ultimate utilization are kinetically complicated. The positron emitter [1-^{11}C]palmitic acid has been investigated as a natural tracer of FFA metabolism by PET (*7,14*). It is suggested that the rapid washout of the tracer is associated with the fatty acid oxidative metabolism (*3,7,14*) and the slower washout with incorporation to myocyte triglyceride pool (*3,7*). Because of distribution of [1-^{11}C]palmitic acid between several tissue pools that turn over at different rates it has been supposed that studies with [1-^{11}C]palmitic acid remain mainly qualitative (*7*). Recently Bergmann et al. (*11*) identified that modeled rates of [1-^{11}C]palmitate utilization with PET correlated closely with directly measured myocardial palmitic acid and total long-chain fatty acid utilization rates.

Fluorine-18-labeled thia-heptadecanoic acid (FTHA) is a new long-chain fatty acid tracer analog and inhibitor of fatty acid metabolism (*15*). Fluorine-18-FTHA has a high first-pass uptake in the heart. After transport into the mitochondria it undergoes initial steps of beta-oxidation and is thereafter trapped in the cell. The rate of radioactivity accumulation in the myocardium is, therefore, believed to reflect the beta-oxidation rate of long-chain fatty acids (*15*). This is supported by the finding that the carnitine palmitoyl-transferase I (CPT I) inhibitor (POCA), which blocks FFA beta-oxidation (*16*), decreased mice cardiac [^{18}F]FTHA uptake by 81% and 87% at 1 and 60 min after tracer injection, respectively (*15*). The tracer has been recently used to study myocardial fatty acid metabolism in humans (*17–19*). Ebert et al. (*17*) found that the distribution of [^{18}F]FTHA in the normal myocardium in the fasting state was homogeneous and the accumulation of tracer increased in response to exercise but was not directly regulated by myocardial blood flow. Altehoefer et al. (*18*) found that [^{18}F]FTHA indicated septal viability better than [^{18}F]fluorodexoyglucose in patients with coronary artery disease (CAD) and left bundle branch block. Contrary to these studies, Schulz et al. (*19*) found that [^{18}F]FTHA uptake was related to 2-methoxyisobutyl isonitrile uptake and that static PET imaging with [^{18}F]FTHA is of limited value when distinguishing between ischemic or hiber-

Received Aug. 6, 1997; revision accepted Nov. 21, 1997.
For correspondence or reprints contact: Maija T. Mäki, MD, Turku PET Centre, University of Turku, FIN-20520, Turku, Finland.

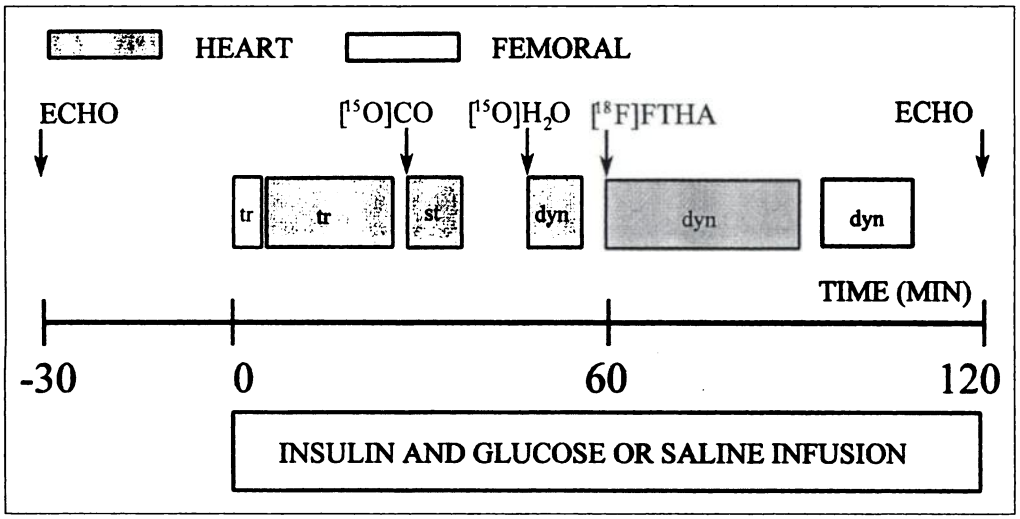

FIGURE 1. Study design. Dyn = dynamic imaging; ECHO = two-dimensional echocradiography; tr = transmission scanning.

nating myocardium and scar. Fluorine-18-FTHA has not been previously used to study FFA uptake in the skeletal muscle.

The purpose of this study was to assess the uptake kinetics of [^{18}F]FTHA in human heart and skeletal muscle and to further investigate the effect of physiological elevation of plasma insulin on tracer uptake. The [^{18}F]FTHA PET studies were performed twice, once in the fasting state and once during insulin clamp in patients with stable CAD.

MATERIALS AND METHODS

Subjects

The study group consisted of 7 male patients (mean age 58 ± 10 yr; mean ejection fraction 58% ± 5%) with stable angiographically confirmed CAD, but no previous myocardial infarction. Since the goal of this study was to assess the kinetics of [^{18}F]FTHA in the normal myocardium the potential effects of CAD on the results were minimized. The angiographic and echocardiographic data were used as previously described to determine normal myocardial segments as precisely as possible (*20*). Each patient gave a written informed consent. The study protocol was accepted by the Ethical Committee of the Turku University Central Hospital.

Study Design

All subjects underwent two dynamic PET studies with [^{18}F]FTHA in random order on consecutive days, once during insulin clamp (n = 6) and once in the fasting state (n = 7) (Fig. 1). The clamp study consisted of a 120-min period of hyperinsulinemia, while saline was infused in the fasting study. Fluorine-18-FTHA was injected at 60 min and dynamic scan of 32 min of the thoracic region was started. Then the femoral region was scanned over 15 min (in the fasting state n = 5 and during hyperinsulinemia n = 6). Myocardial blood volume and blood flow were determined with [^{15}O]CO and [^{15}O]H_2O before the [^{18}F]FTHA study in the fasting state. Heart rate and blood pressure were monitored during the studies to calculate the rate-pressure product. Electrocardiogram was continuously monitored during the PET study. Echocardiograms were obtained immediately before and after the PET studies to assess the potential wall motion abnormalities.

Infusions and Blood Sampling

Two catheters were placed, one in an antecubital vein for infusion of saline or glucose and insulin and for tracer injection and one in a radial vein of the contralateral hand that was warmed (air temperature 70°C) for sampling of arterialized venous blood. In the clamp study, an intravenous primed continuous insulin infusion was started as previously described (*20,21*). The rate of insulin infusion was 1 mU/kg/min. During hyperinsulinemia, euglycemia was maintained by infusing 20% glucose. The rate of the glucose infusion was adjusted according to plasma glucose concentrations measured every 5–10 min from arterialized venous blood. Serum FFA, insulin and lactate concentrations were determined every 30 min. Twenty-three blood samples were taken to measure total ^{18}F radioactivity with the well counter (Bicron 3MW3/3P; Bicron, Inc., Newbury, OH). Blood samples to measure radioactive [^{18}F]FTHA metabolites were drawn at 2 min, then every 5 min until 30 min and thereafter every 10 min to the end of the study.

PET: Production of [^{15}O]CO and [^{15}O]H_2O

For production of [^{15}O] a low-energy deuteron accelerator Cyclone 3 was used (Ion Beam Application, Inc., Louvain-la-Neuve, Belgium). Oxygen-15-CO was produced in a conventional way (*22*). Oxygen-15-H_2O was produced using dialysis techniques in a continuously working water module (*23*). Sterility and pyrogenity tests for water and chromatographic analysis for gases were performed to verify the purity of the products.

Production of Fluorine-18-FTHA

For nucleophilic radiofluorination the benzyl 14(R,S)-tosyloxy-6-thia-heptadecanoate was synthesized from 8-bromo-1-octanol (*24*). Product was isolated as a colorless oil by flash chromatography (hexane/ethylacetate;3:1). H-NMR spectra showed δ_H ($CDCl_3$); 0.82 (t, 3 H, -CH_3), 1.25 (m, 12 H,-CH2-), 1.55 (m, 10 H, -CH_2-), 2.44 (s, 3 H, Ar-CH_3), 2.36–2.52 (m, 4 H, -CH_2-S-CH_2-), 4.55 (q, 1 H, CH-OTs), 5.12 (s, 2 H, -CO_2-CH_2-Ar), 7.3–7.4 (m, 7 H, ArH), 7.8 (d, 2 H, ArH). The precursor solution (3 mg in 1 ml acetonitrile) was added into dry Kryptofix 222/K_2CO_3-$^{18}F^-$-residue. After the reaction of 10 min at 90°C the reaction mixture was evaporated and 0.2 *M* KOH was added for hydrolyzis (Fig. 2). After neutralization with acetic acid the product 14(R,S)-[^{18}F]FTHA was purified with radio high-performance liquid chromatography (HPLC) on a μ Bondapak C_{18} column using methanol:water: acetic acid (85:15:0.4) as eluent at a flow rate of 3.0 ml/min. The [^{18}F]FTHA fraction was collected, evaporated and dissolved to 4% human serum albumin and filtrated (0.22 μm Cathivex; Millipore Corp., Bedford, MA). The radiochemical yield at the end of synthesis was 45% ± 10% and the radiochemical purity of the final product was > 98%. The chemical purity was confirmed with liquid chromatography-mass spectrometry analysis.

Image Acquisition, Processing and Corrections

The patients were positioned supine in an 15-slice ECAT 931/08-12 tomograph (Siemens/CTI, Inc., Knoxville, TN) with a measured axial resolution of 6.7 mm and 6.5 mm in-plane. To correct for photon attenuation, transmission scanning was performed for 5 min for femoral regions and 20 min for thoracic

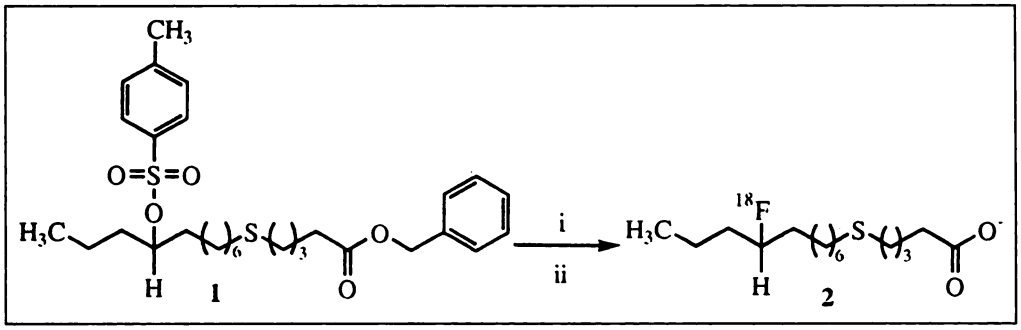

FIGURE 2. Synthesis of 14(R,S)-[^{18}F]FTHA (2) from benzyl 14(R,S)-tosyloxy-6-thia-heptadecanoate (1). (i) Kryptofix 2.2.2, CH_3CN, K_2CO_3, [^{18}F]F^-; (ii) 0.2 M KOH, 95°C.

regions before the emission scans. The myocardial flow study was performed as previously described (*25*) in the fasting state. The mean doses of [^{15}O]CO and [^{15}O]H_2O were 3780 ± 460 MBq and 1720 ± 130 MBq, respectively. Thereafter 190 ± 16 MBq [^{18}F]FTHA was injected intravenously over 30 sec (200 ± 7 MBq in the clamp study and 180 ± 25 MBq in the fasting study, ns). Dynamic scanning of the cardiac region was started simultaneously for 32 min (12 × 15 sec, 4 × 30 sec, 2 × 120 sec, 1 × 180 sec and 4 × 300 sec). Dynamic imaging of femoral regions was started for 15 min (5 × 180 sec). All data were corrected for deadtime, decay and photon attenuation and reconstructed in a 128 × 128 matrix. The final in-plane resolution in reconstructed and Hann-filtered (0.3 cycles/pixel) images was 9.5 mm FWHM.

Fluorine-18-FTHA Metabolite Analysis

Serum metabolite samples were deproteinizated by methanol and centrifugated. From the supernatant fraction the nonmetabolized [^{18}F]FTHA was analyzed by HPLC on a μ Bondapak C_{18} column using methanol:water:acetic acid (85:15:0.4) as eluent at a flow rate of 3.0 ml/min. The radioactivity on the column outlet flow was monitored with a coincidence probe consisting of two 3 × 3 NaI crystals. The metabolite analysis was not successful in 2 patients in the fasting state and 1 patient during insulin clamp for technical reasons. Since the nonmetabolized fraction of the tracer was quite comparable between the patients (Fig. 3), the input function was corrected with the mean metabolite fraction in those studies.

Definition of Regions of Interest in PET Studies

Transaxial PET slices were visually aligned and the left ventricular myocardium was assigned to eight segments (anterobasal, anterior septal, anterior, lateral, posterior septal, apical, posterobasal and inferior) with the help of a heart map phantom (*20*). Thirty-four to 30 elliptical regions of interest (ROIs) were placed on an average nine transaxial ventricular slices in each [^{18}F]FTHA study, with care taken to avoid myocardial borders. A mean of 17 elliptical ROIs were drawn in representative transaxial ventricular slices in the flow study. The larger ROIs were used in the flow study to enhance the accuracy of the measurements. For the femoral regions ROIs were drawn on the anteromedial, anterolateral and posterior muscle compartments (*26*) in four adjacent planes. Large vessels were avoided when outlining the muscle areas.

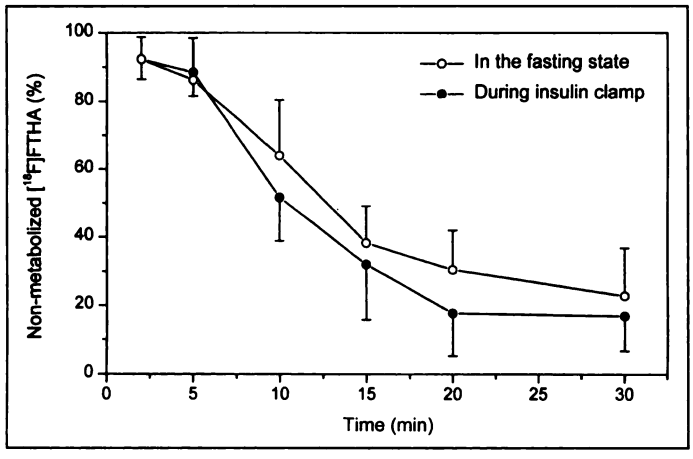

FIGURE 3. Percentage of nonmetabolized [^{18}F]FTHA in blood by high-performance liquid chromatography expressed as a function of time. The metabolites of [^{18}F]FTHA appeared rapidly to blood, and after 15 min the majority of blood radioactivity was in metabolites both in the fasting state and during insulin clamp. The plasma radioactivity curves in each patient were corrected using the data about metabolite fractions.

Calculation of the Regional Fluorine-18-FTHA Fractional Uptake Constant and FFA Uptake Index

The nonmetabolized fraction of [^{18}F]FTHA was used to correct the plasma input function. In femoral regions, blood background was subtracted using average blood volume of 3% (*26*). Thereafter, plasma, myocardial and femoral tissue time-activity curves were analyzed graphically (*27*) with the equation:

$$\frac{C_t(T)}{C_p(T)} = K_i \frac{\int_0^T C_p(t)dt}{C_p(T)} + V_d, \qquad \text{Eq. 1}$$

where $C_t(T)$ corresponds the radioactivity concentration in tissue at time T, $C_p(T)$ the plasma radioactivity concentration at time T and V_d the distribution volume of the tracer. When $C_t(T)/C_p(T)$ is plotted against the integral of plasma time-acitivity curve divided by $C_p(T)$ (the normalized plasma time) the slope of the plot in the graphical analysis is equal to the fractional uptake constant of [^{18}F]FTHA, K_i. The last seven time points (6–29.5 min) were used to determine the slope by linear regression in the myocardium (Fig. 4A and B) and all 5 time points were used in the femoral regions (Fig. 4C and D). Since Ki is representing the fraction of tracer taken up by tissues during time from actual circulating substrate amount, the myocardial and skeletal muscle FFA uptake indices were calculated by multiplying myocardial and skeletal muscle K_i with the mean serum FFA concentration during PET imaging. The lumped constant (LC) for [^{18}F]FTHA was assumed to be 1.0.

Coronary Angiography and Echocardiography

All patients underwent selective coronary angiography by standard techniques. A significant lesion was defined as that compromising the luminal diameter by 50% or more. The cine tapes were analyzed by an experienced radiologists. Digitized two-dimensional echocardiography (Acuson 128XP/5; Acuson Inc., Mountain View, CA) was performed according to standard protocols (*28*) and previously described modifications (*20*). Echocardiograms were analyzed by an experienced physician blinded to both PET and clinical data. Normal wall motion was defined as ≥ 5 mm of endocardial excursion and systolic thickening and no wall thinning (the segments were considered to be thinned if the wall thickness was reduced by > 25% compared with the adjacent normal segments).

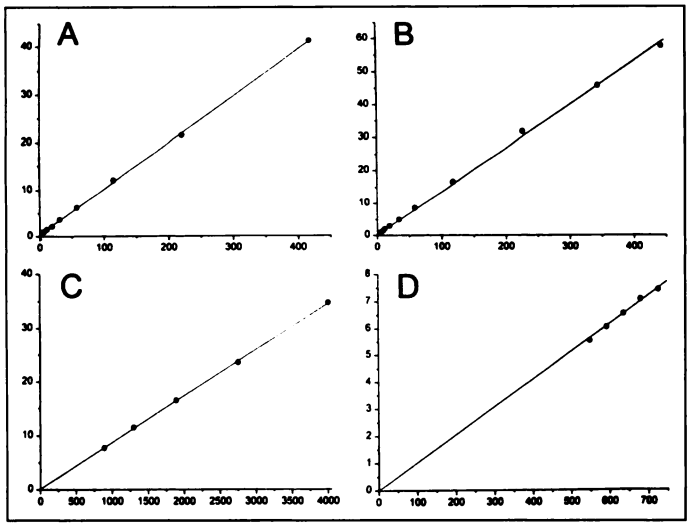

FIGURE 4. Examples of graphical analysis plots of myocardial and femoral muscles. A and C display myocardial and skeletal muscle plots in the fasting state. B and D show the respective plots during insulin clamp. All plots show linear increase indicating metabolic trapping. The label for the y axis is $C_t(T)/C_p(T)$ and for the x axis normalized plasma time in minutes.

Normal Myocardial Segments. Angiographic and echocardiographic data were localized to the segmental heart map phantom designed for our studies as previously described (*20*). Only normal myocardial segments (no abnormality in echocardiography and angiography stenosis ≤ 50%) were accepted. Finally, 25 normal myocardial segments (range 2–5 per patient, same 25 segments in the fasting and clamp study) in the 7 patients were included.

Analytical Procedures. Serum FFAs were determined by an enzymatic method (ACS-ACOD Method; Wako Chemicals GmbH, Neuss, Germany) and serum insulin was measured by radioimmunoassay kit (Pharmacia, Uppsala, Sweden). Plasma glucose was determined in duplicate by the glucose oxidase method (*29*) using an Analox GM7 (Analox Instruments LTD, London, England) glucose analyzer. Lactate was measured by enzymatic analysis (*30*).

Statistical Analysis. All results are expressed as mean value and s.d. The difference between the fasting state and during insulin clamp was statistically tested using a paired comparisons Student's t-test. P values < 0.05 were interpreted as statistically significant. The statistical computation was performed with the SAS statistical program package (SAS Institute, Inc., Gary, NC).

RESULTS

Metabolic and Physiologic Characteristics During the Studies

Plasma glucose concentrations were similar in the fasting state and during hyperinsulinemia (Table 1). During hyperinsulinemia serum FFA concentrations decreased by 80% ($p < 0.01$) and plasma lactate concentrations increased slightly ($p < 0.05$) as compared to the fasting state. The rate-pressure products were comparable during the two occasions. No patient experienced chest pain or showed ischemic electrocardigram changes during the PET studies. No alterations in wall motion was observed by echocardiography between the two studies. In 6 patients, the normal segments located in the inferoposterior and lateral wall and in 1 patient to the anterior, anteroseptal, apical and lateral wall.

Myocardial Blood Flow in the Normal Myocardium

In those myocardial segments that were classified as normal according to angiography and echocardiography the PET-derived myocardial blood flow using was normal (0.81 ± 0.14 ml/g/min, range 0.69–1.1 ml/g/min).

Myocardial Fluorine-18-FTHA Kinetics and FFA Uptake Indices in the Fasting State and During Insulin Clamp

Rapid tracer uptake was identified in the myocardium within 2–3 min after [^{18}F]FTHA injection and it remained nearly constant during the next 30 min (Fig. 5). Myocardium-to-blood radioactivity ratios at 27–32 min after tracer injection were 12 ± 6 in the fasting state and 19 ± 8 ($p < 0.05$) during hyperinsulinemia leading to excellent myocardial image quality (Fig. 6A and B). The metabolites of [^{18}F]FTHA appeared in blood within a few minutes after injection and their fraction steadily increased (Fig. 3). At 20–30 min about 70%–80% of blood radioactivity was in metabolites (Fig. 3). In the graphical analysis the plots were linear, indicating metabolic trapping (Fig. 4). The mean K_i values in the fasting state and during insulin clamp in the normal myocardial regions were 0.11 ± 0.04 ml/g/min and 0.12 ± 0.03 ml/g/min (ns). Although the K_i values were similar during both approaches there was high variability between the subjects (Fig. 7). The mean FFA uptake indices decreased by 76% during insulin clamp (5.8 ± 1.7 μmol/100 g/min in the fasting state and 1.4 ± 0.5 μmol/100 g/min during insulin clamp, $p < 0.005$).

Femoral Muscle Fluorine-18-FTHA Kinetics and FFA Uptake Indices. The femoral muscles were clearly visualized in both studies (Fig. 6C and D). Femoral [^{18}F]FTHA uptake plots showed also a linear increase, indicating metabolic trapping (Fig. 4C and D). The average femoral muscle fractional [^{18}F]-FTHA uptake rate was lower (0.0071 ± 0.0014 ml/g/min) in the fasting state than during insulin clamp (0.0127 ± 0.0036 ml/g/min, $p < 0.05$). However, the calculated FFA uptake indices were about three times higher in the fasting state (0.38 ± 0.09 μmol/100 g/min) compared to that during insulin clamp (0.12 ± 0.05 μmol/100 g/min, $p < 0.005$).

DISCUSSION

The purpose of this study was to apply a new tracer, [^{18}F]FTHA, and PET to investigate uptake of FFAs in the normal myocardium and femoral muscle and further to deter-

TABLE 1
Metabolic and Physiologic Characteristics During PET Studies

	P-glucose (mmol/liter)	S-insulin (mU/liter)	S-FFA (μmol/liter)	P-lactate (mmol/liter)	RPP
Fasting state	5.3 ± 0.4	8 ± 3	560 ± 80	0.9 ± 0.5	7270 ± 1340
During clamp	5.4 ± 0.8	62 ± 10†	110 ± 30*	1.1 ± 0.2*	6160 ± 660

*$p < 0.01$.
†$p < 0.001$.
FFA = free fatty acid; P = plasma; RPP = rate pressure product; S = serum.

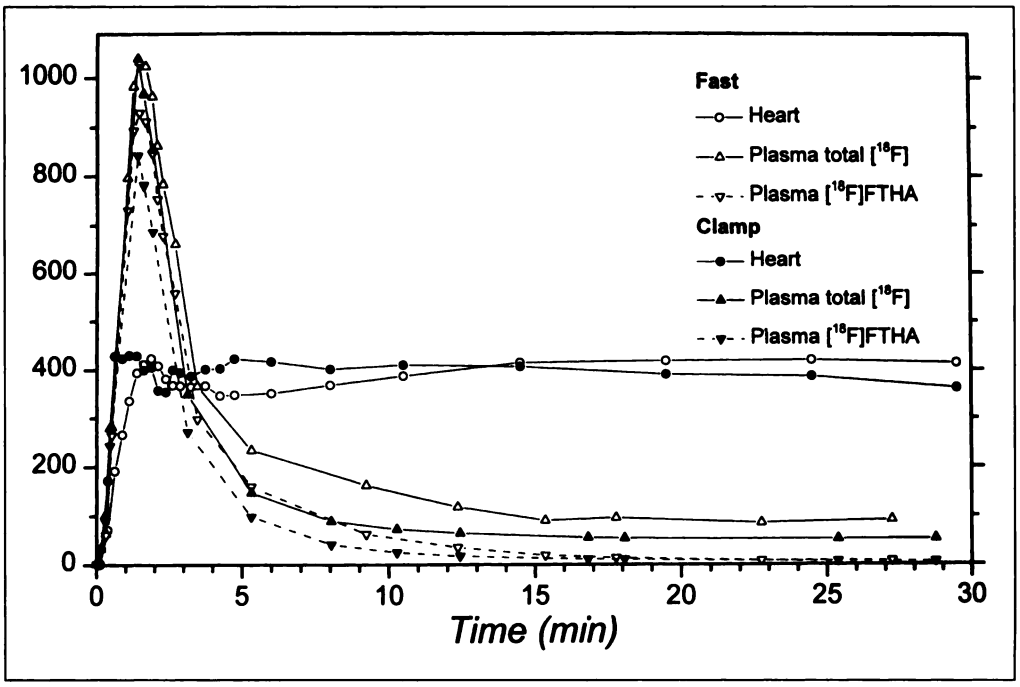

FIGURE 5. Example of heart and plasma radioactivity curves as a function of time in the fasting state ([^{18}F]FTHA dose 195 MBq) and during insulin clamp ([^{18}F]FTHA dose 193 MBq). Solid lines with triangles = plasma total radioactivity curves; dashed lines = curves corrected for blood metabolites.

mine their response to insulin stimulation, which is known to suppress FFA uptake (*5,9,12*) and oxidation (*5*) in muscle tissue. The image quality was excellent and the graphical analysis was successfully applied both in the cardiac and femoral muscle. When a simple model for estimation of FFA uptake was applied the myocardial and femoral muscle uptake rates in the fasting state were concordant with the previous studies (*5,9,11,12,31–33*). Insulin suppressed myocardial FFA uptake by 76% and femoral muscle FFA uptake by 68%.

PET Image Quality and Tracer Kinetics

Rapid tracer uptake was identified in the myocardium, leading to excellent image quality in the heart both in the fasting state and during insulin clamp (Fig. 6A and B). In addition, the femoral muscles were clearly visualized in both study conditions (Fig. 6C and D). The finding that fractional tracer uptake values in the heart during insulin stimulation were close to those obtained in the fasting state is somewhat surprising. The fractional tracer uptake represents the fraction of tracer taken up

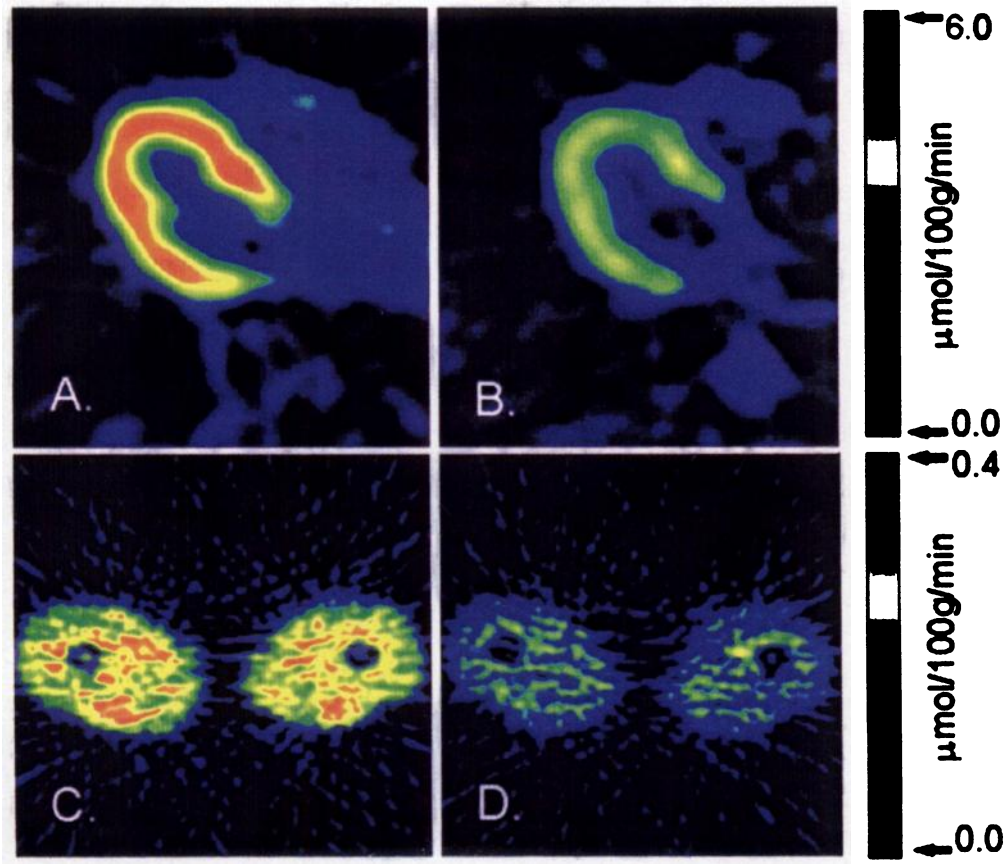

FIGURE 6. Examples of parametric images measured with [^{18}F]FTHA. Myocardial midventricular transaxial slice and cross-section of femoral region measured in the fasting state (A,C) and during insulin clamp (B,D) in the same subject.

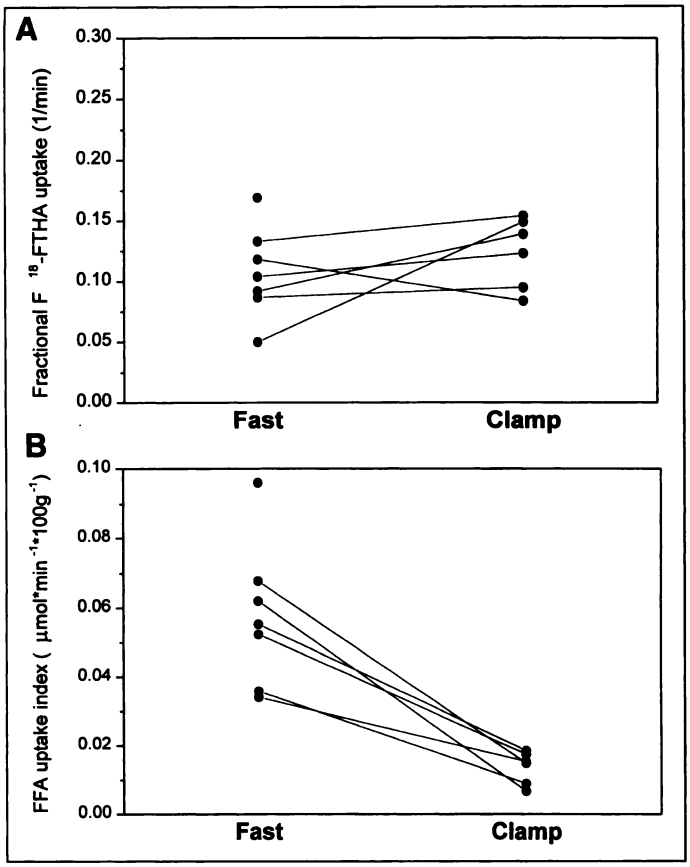

FIGURE 7. (A) Myocardial fractional [^{18}F]FTHA uptake values (K_i) and (B) FAA uptake indices in each subject in the fasting state and during insulin clamp. Although K_i values were similar during both approaches there was variability between subjects.

by tissues during time from actual circulating substrate amount and is related to substrate extraction fraction when flow is not changed. Insulin is known to reduce net FFA utilization in cardiac (*9,11*) and skeletal muscle (*5,12*). Uptake of total FFAs by the myocardium is directly related to their concentration in plasma (*3*) and, on the other hand, the mechanism of insulin action on FFAs can be suggested to be mainly indirect (reduction of serum FFA concentrations due to inhibition of peripheral lipolysis) (*8*) leading to rather constant fractional uptake rates in a wide range of serum FFA concentrations. There was, however, large interindividual variability in the fractional uptake values (Fig. 7). Therefore, myocardial FFA uptake cannot be directly derived from the circulating FFA concentrations. The mean fractional uptake rate constant K_i in our study in the myocardium in the fasting state was similar to the values obtained by Ebert et al. (*17*) in healthy young men using the same tracer.

In the skeletal muscle the fractional tracer uptake was even higher during hyperinsulinemia as compared to fasting state, suggesting that during lower circulating FFA levels larger part of it is taken up by muscle. This is concordant with the previous reports (*5,12*) showing that FFA extraction fraction is increased with decreased blood FFA concentrations. Since fractional tracer uptake is also related to image quality, this phenomenon explains the excellent image quality obtained during the two approaches.

General Features of the Measurement of FFA Uptake and Metabolism

Measuring the uptake of a substrate by the heart and skeletal muscle does not indicate whether the substrate is immediately oxidized or stored for later metabolism. Therefore, the accumulation of a FFA tracer in the tissue probes the net utilization rate of long-chain FFAs, the sum of esterification and oxidation (*15*). The FFA is activated to fatty acyl-CoA, which is either transported to mitochondria for oxidation, stored as triglycerides or transformed to structural lipids (*1,3,7*). In the myocardium 80%–84% of the FFAs extracted undergo rapid oxidation and only a small fraction is entering the intracellular lipid pool in the fasting state (*11,33,34*). However, during glucose infusion the fraction undergoing rapid oxidation may decrease. In contrast to myocardium, in skeletal muscle FFA enter large premitochondrial triglyceride fatty acid pools before oxidation (*4*). This yields to a delay in entry of FFA from plasma into the oxidative pathways. Furthermore, another known problem in measuring FFA oxidation with tracer technique is that the rate of estimated FFA oxidation is slightly underestimated, because part of oxidation is from unlabeled storage form (*34*). For example Nellis et al. (*34*) have estimated that about 20% of myocardial fatty acid oxidation is from unlabeled storage.

Fluorine-18-FTHA as a Tracer for FFA Uptake

The general features of the measurement of FFA metabolism are of course valid also for [^{18}F]FTHA. However, [^{18}F]FTHA is a radiolabeled long-chain fatty acid analog designed to undergo metabolic trapping because complete beta-oxidation of the chain is blocked by the sulfur heteroatom. Otherwise it is expected to follow the same metabolic pathways as physiologic FFAs. Fluorine-18-FTHA is rapidly transported and metabolized in heart and has been believed to provide information on the rate of substrate delivery for beta-oxidation of the myocardium (*15*). Tissue [^{18}F]FTHA uptake was shown not to be directly regulated by myocardial blood flow rate but rather increases when myocardial energy demands are increased, e.g., during exercise (*17*). Pretreatment with the carnitine POCA, which selectively blocks fatty acid beta-oxidation (*16*), decreased cardiac [^{18}F]FTHA uptake in mice by 81% and 87% at 1 and 60 min, respectively (*15*). These findings suggest that the accumulation of [^{18}F]FTHA in the normal myocardium is mainly associated with FFA beta-oxidation and only 5%–10% is esterified.

Fluorine-18-FTHA has certain advantages as compared with ^{11}C-palmitate. Intracellular trapping of [^{18}F]FTHA has been described without redistribution (*15*), resulting in a more simple model for data analysis. Labeling with ^{18}F with longer physical half-life allows simple acquisition and calculation and the image quality is good. However, [^{18}F]FTHA is a rather new tracer and until now only a few studies have been published (*15–19*). The metabolic handling of FTHA along the beta-oxidation pathway and the subsequent formation of protein-bound metabolites have not been studied and fully characterized in different physiological and pathophysiological conditions. Therefore, in this study, we interpreted the results to represent fatty acid uptake rather than FFA beta-oxidation.

FFA Uptake in the Myocardium

Quantitation of myocardial fatty acid utilization has been previously based on invasive determination of arteriovenous concentration differences and simultaneous myocardial blood flow measurements in animals. Using this method, myocardial total FFA uptake in fasted dogs has varied from 6.6–21.7 µmol/100 g/min (*9,11,31,32*). In a study by Bergmann et al. (*11*), myocardial FFA utilization was quantitated using [^{11}C]palmitate and PET. In that study PET-derived rates of palmitate utilization correlated closely with directly measured myocardial palmitate (2.7 µmol/100 g/min) and total long-

chain fatty acid utilization rates (10.7 μmol/100 g/min) in fasted dogs (*11*).

Although different long-chain fatty acids are extracted and used by the myocardium to a different extent (*7,11*), the extraction proportion of each individual FFA remained relatively constant during interventions (glucose-insulin infusion) (*11*). Therefore, the total FFA utilization can be calculated if the percentage of given fatty acid to total FFA utilization is known (*11*). For example, palmitate represents 24.5%–27% of arterial fatty acids in the fasting state and its uptake rate is 1.3–2.7 μmol/100 g/min (*11,32*), which accounts for approximately 20%–23% of all fatty acids used by the myocardium (*11,32*). Taking into consideration the previously measured palmitate uptake rates, percentage of palmitate use of all FFAs and that in the myocardium 84% of extracted FFAs undergo rapid oxidation in the fasting state (*11,33*) the calculated myocardial FFA uptake would be 5.7–13.5 μmol/100 g/min and beta-oxidation 4.8–11.3 μmol/100 g/min in the fasting state (*11,32*). The [^{18}F]FTHA-derived myocardial FFA uptake rate in the fasting state in this study (5.8 μmol/100 g/min) is in concordance with the previous reports. In our study, during euglycemic hyperinsulinemia, the myocardial FFA uptake indices decreased by 76%. This finding is concordant with a previous study in dogs, in which insulin clamp technique (~73 μU/ml) was combined with arterial and coronary sinus blood sampling and myocardial FFA uptake was decreased by 95% (*9*).

Fatty Acid Uptake in Skeletal Muscle in Humans

This study tried to measure fatty acid metabolism directly in skeletal muscle by PET. The image quality was reasonably good and resulted in acceptable count statistics for the graphical analysis. The femoral muscle FFA uptake rates in this study in the fasting state (0.38 μmol/100 g/min) are similar to what Kelley et al. (*5*) detected using leg balance technique (0.39 μmol/min/100 ml of leg tissue). Our results also are of the same magnitude with invasive measurements of forearm FFA uptake rate (0.25 μmol/min/100 ml) (*12*) and oleate uptake rate (0.38 μmol/min/100 ml) (*4*) considering that in the latter study the arterial FFA concentrations were double as high as in our study. During hyperinsulinemia in this study, femoral muscle FFA uptake was 0.12 ± 0.05 μmol/100 g/min, which is also very similar to the previous measurements (0.11–0.09 μmol/min/100 ml) (*5,12*).

In the present PET method, the tracer kinetics are visualized and quantitated in a region of limb that can easily be identified as muscle tissue. The anteriovenous balance method is able to give estimates of substrate utilization in the whole limb, not in the specific tissue region. If muscle values are estimated the muscle mass of the limb is usually assumed rather than measured as is the fraction of blood flow that flows through muscle tissue. The present method using PET does not require blood flow information and the methodological problems that might be caused by flow measurement do not confound the quantitation of FFA uptake.

Study Limitations

In this study, cardiac tracer uptake was measured in the normally perfused and normally functioning myocardial regions in the patients with stable CAD and preserved global left ventricular ejection fraction. Although all efforts were made to eliminate the confounding effects of coronary heart disease, we cannot completely exclude that it might have affected the measured [^{18}F]FTHA kinetics. However, similar [^{11}C]palmitate clearance rates (representing FFA beta-oxidation) have been identified in the normal myocardial regions of CAD patients and in normal subjects (*14*). In this study, a simple model for estimations of FFA uptake was applied. The fractional [^{18}F]FTHA uptake values derived from graphical analysis of [^{18}F]FTHA kinetics were multiplied by actual serum total FFA concentration and the result was assumed to represent uptake of all FFAs in the myocardium and skeletal muscle. This model is based on two assumptions: First, the fraction of [^{18}F]FTHA used from blood is similar to that of other FFAs and, second, the proportion of [^{18}F]FTHA used is not changed by insulin or changes in serum fatty acid concentrations.

CONCLUSION

Fluorine-18-FTHA PET appears to be a feasible method to estimate fatty acid kinetics in myocardial and skeletal muscle. The fractional tracer uptake into these tissues appears to be adequate both in the fasting state and during insulin stimulation. Furthermore, physiologically reasonable estimations of myocardial FFA uptake were obtained and the uptake rates were suppressed in response to insulin. In the femoral muscle, the FFA uptake rates were in concordance with the previous studies both in the fasting state and during hyperinsulinemia. However, the kinetics of [^{18}F]FTHA along the metabolic pathways and the formation of protein-bound metabolites in different pathophysiological conditions still wait for further studies.

ACKNOWLEDGMENTS

We thank the technologists in the Turku PET Centre for their skill and dedication throughout this study. We also thank Tuula Tolvanen, MSc, Hannu Sipilä, MSc, and Mika Teräs, MSc, for their excellent technical assistance. The study was supported by the grants of Finnish Foundation for Cardiovascular Research, Maud Kuistila Foundation, Orion Farmos Foundation and Turku University Foundation.

REFERENCES

1. Neely J, Morgan H. Relationship between carbohydrate and lipid metabolism and the energy balance of heart muscle. *Annu Rev Physiol* 1974;36:413–459.
2. Opie LH, Owen P, Riemersma R. Relative rates of oxidation of glucose and free fatty acids by ischaemic and non-ischaemic myocardium after coronary artery ligation in the dog. *Eur J Clin Invest* 1973;19:419–435.
3. Taegtmeyer H. Energy metabolism of the heart: from basic concepts to clinical applications. *Curr Probl Cardiol* 1994;19:62–113.
4. Dagenais G, Tancredi R, Zierler K. Free fatty acid oxidation by forearm muscle at rest, and evidence for an intramuscular lipid pool in the human forearm. *J Clin Invest* 1976;58:421–431.
5. Kelley D, Mokan M, Simoneau J-A, Mandarino L. Interaction between glucose and free fatty acid metabolism in human skeletal muscle. *J Clin Invest* 1993;92:91–98.
6. Kelley D, Simoneau J-A. Impaired free fatty acid utilization by skeletal muscle in non-insulin-dependent diabetes mellitus. *J Clin Invest* 1994;94:2349–2356.
7. Schelbert H, Schwaiger M. PET studies of the heart. In: Phelps M, Marizziotta J, Schelbert H, eds. *Positron emission tomography and autoradiography: principles and applications for the brain and heart*. New York: Raven Press; 1986:599–616.
8. Fain J, Kovacev V, Scow R. Antilipolytic effect of insulin in isolated fat cells of the rat. *Endocrinology* 1966;78:773–778.
9. Barrett E, Schwartz R, Francis C, Zaret B. Regulation by insulin of myocardial glucose and fatty acid metabolism in the conscious dog. *J Clin Invest* 1984;74:1073–1079.
10. Randle P, Garland P, Hales C, Newsholme E. The glucose fatty acid cycle: its role in insulin sensitivity and the metabolic disturbances of diabetes mellitus. *Lancet* 1963; 1:785–789.
11. Bergmann S, Weinheimer C, Markham J, Herrero P. Quantitation of myocardial fatty acid metabolism using PET. *J Nucl Med* 1996;37:1723–1730.
12. Capaldo B, Napoli R, Di Marino L, Picardi A, Riccardi G, Sacca L. Quantitation of forearm glucose and free fatty acid (FFA) disposal in normal subjects and type II diabetic patients: evidence against an essential role for FFA in the pathogenesis of insulin resistance. *J Clin Endocrinol Metab* 1988;67:893–898.
13. Liedtke J. Alterations of carbohydrate and lipid metabolism in the acutely ischemic heart. *Prog Cardiovasc Dis* 1981;23:321–336.
14. Tamaki N, Kawamoto M, Takahashi N, et al. Assessment of myocardial fatty acid metabolism with positron emission tomography at rest and during dobutamine infusion in patients with coronary artery disease. *Am Heart J* 1993;125:702–710.
15. DeGrado T, Coenen H, Stöcklin G. 14 (R,S)-[^{18}F]fluoro-6-thia-heptadecanoic acid (FTHA): evaluation in mouse of a new probe of myocardial utilization of long chain fatty acids. *J Nucl Med* 1991;32:1888–1896.
16. Rosen P, Reinauer H. Inhibition of carnitine palmitoyltransferase by phenylalkyloxiranecarboxylic acid and its influence on lipolysis and glucose metabolism in isolated perfused hearts of streptozotocin-diabetic rats. *Metabolism* 1984;33:177–185.

17. Ebert A, Herzog H, Stöcklin G, et al. Kinetics of 14(R,S)-fluorine-18-fluoro-6-thia-heptadecanoic acid in normal human hearts at rest, during exercise and after dipyridamole injection. *J Nucl Med* 1994;35:51–56.
18. Altehoefer C, vom Dahl J, Bares R, Stocklin GL, Bull U. Metabolic mismatch of septal beta-oxidation and glucose utilization in left bundle branch bloc assessed with PET. *J Nucl Med* 1995;36:2056–2059.
19. Schultz G, vom Dahl J, Kaiser H, et al. Imaging of β-oxidation by static PET with 14(R,S)-[^{18}F]-fluoro-6-thiaheptadecanoic acid (FTHA) in patients with advanced coronary heart disease: a comparison with ^{18}FDG PET and ^{99m}Tc-MIBI SPET. *Nucl Med Commun* 1996;17:1057–1064.
20. Knuuti MJ, Nuutila P, Ruotsalainen U, et al. Euglycemic hyperinsulinemic clamp and oral glucose load in stimulating myocardial glucose utilization during positron emission tomography. *J Nucl Med* 1992;33:1255–1262.
21. DeFronzo R, Tobin J, Andres R. Glucose clamp technique: a method for quantifying insulin secretion and resistance. *Am J Physiol* 1979;237:E214–E223.
22. Clark J, Crouzel C, Meyer G, Strijckmans K. Current methodology for oxygen-15 production for clinical use. *Appl Radiat Isot* 1987;38:597–600.
23. Crouzel C, Clark J, Brihaye C, et al. Radiochemistry automation for PET. In: Stöcklin G, Pike V, eds. *Radiopharmaceuticals for positron emission tomography*. Dordrecht, The Netherlands: Kluwer Academic Publishers; 1993:45–90.
24. DeGrado T. Synthesis of 14(R,S)-[^{18}F]fluoro-6-thia-heptadecanoic acid (FTHA). *J Lab Compd Radiopharm* 1991;24:889–995.
25. Mäki M, Luotolahti M, Nuutila P, et al. Glucose uptake in the chronically dysfunctional but viable myocardium. *Circulation* 1996;93:1658–1666.
26. Raitakari M, Knuuti J, Ruotsalainen U, et al. Insulin increases blood volume in human skeletal muscle:studies using [^{15}O]CO and positron emission tomography. *Am J Physiol* 1995;269:E1000–E1005.
27. Patlak CS, Blasberg RG. Graphical evaluation of blood-to-brain transfer constants from multipletime uptake data. Generalizations. *J Cereb Blood Flow Metab* 1985;5: 584–590.
28. Schiller N, Shah P, Crawford M, et al. Recommendations for quantitation of the left ventricle by two-dimensional echocardiography. *J Am Soc Echocardiogr* 1989;2:358–367.
29. Kadish A, Little R, Sternberg J. A new and rapid method for the determination of glucose by measurement of rate of oxygen consumption. *Clin Chem* 1968;14:116–131.
30. Marbach E, Weil M. Rapid enzymatic measurement of blood lactate and pyruvate. *Clin Chem* 1967;13:314–325.
31. Fox K, Abendschein D, Ambos H, Sobel B, Bergmann S. Efflux of metabolized and nonmetabolized fatty acid from canine myocardium. Implications for quantifying myocardial metabolism tomographically. *Circ Res* 1985;57:232–243.
32. van der Vusse G, Roemen Th, Prinzen F, Coumans W, Reneman R. Uptake and tissue content of fatty acids in dog myocardium under normoxic and ischemic conditions. *Circ Res* 1982;50:538–546.
33. Wisneski J, Gertz E, Neese R, Mayr M. Myocardial metabolism of free fatty acids. Studies with ^{14}C-labeled substrates in humans. *J Clin Invest* 1987;79:359–366.
34. Nellis S, Liedtke A, Renstom B. Fatty acid kinetics in aerobic myocardium: characteristics of tracer carbon entry and washout and influence of myocardial demand. *J Nucl Med* 1992;33:1864–1874.

Quantitation of Presynaptic Cardiac Sympathetic Function with Carbon-11-Meta-Hydroxyephedrine

James H. Caldwell, Keith Kroll, Zheng Li, Katherine Seymour, Jeanne M. Link and Kenneth A. Krohn
Division of Cardiology and Departments of Bioengineering and Radiology, Veterans Administration Medical Center, and the University of Washington, Seattle, Washington

The purpose of this study was to validate an axially distributed blood–tissue exchange model for the quantitation of cardiac presynaptic sympathetic nervous system function that could be applied to PET images. The model accounts for heterogeneity in myocardial blood flow, differences in transport rates of ^{11}C-meta-hydroxyephedrine (mHED) across the capillary endothelium and/or neuronal membranes, the virtual volumes of distribution in the interstitial space and neuron and retention of mHED in the neuronal vesicles. **Methods:** Multiple indicator outflow dilution and residue detection methods were used to measure the kinetics of radiolabeled intravascular space and interstitial space markers and ^{11}C-mHED in isolated perfused rat heart at baseline and during norepinephrine neuronal transporter blockade with desipramine (DMI). The outflow dilution and residue detection data were modeled with a multiple pathway, four-region, axially distributed model of blood–tissue exchange describing flow in the capillary and exchange between regions using permeability-surface area products with units of clearance of milliliters per minute per gram. Meta-hydroxyephedrine may enter the nerve terminal via membrane transport, where it may be sequestered by first-order unidirectional uptake within vesicles. Release of mHED from the vesicles is modeled via exchange with the interstitial space. **Results:** After intracoronary injection, mHED transport across the capillary endothelium and in the interstitial space closely followed that of sucrose. Subsequently, mHED was retained in the heart, whereas sucrose washed out rapidly. With DMI the outflow dilution curves more closely resembled those of sucrose. Model parameters reflecting capillary-interstitial kinetics and volumes of distribution were unchanged by DMI, whereas parameters reflecting the neuronal transporter process and volumes of distribution in the nerve terminal and vesicular sequestration were markedly decreased by DMI. Application of the model to a pilot set of canine PET images of mHED suggests the feasibility of this approach. **Conclusion:** Meta-hydroxyephedrine kinetics in the heart can be quantitated using an axially distributed, blood–tissue exchange model that accounts for heterogeneity of flow, reflects changes in neuronal function and is applicable to PET images.

Key Words: sympathetic nervous system; PET; modeling; meta-hydroxyephedrine; neuronal transporter

J Nucl Med 1998; 39:1327–1334

Substantial and increasing evidence supports the concept that aberrations in cardiac sympathetic nervous system (SNS) function contribute to and may be primarily responsible for the morbidity and mortality associated with cardiac conditions such as sudden cardiac death (*1*), congestive heart failure (*2–4*) and post-myocardial infarction depression (*5,6*). A major limitation to understanding the role of the SNS in these conditions has been the absence of quantitative methods for noninvasive examination of global and/or regional pre- and postsynaptic cardiac SNS function.

The distribution and retention in the myocardium of norepinephrine (NE) analogs (*7–9*) and the postsynaptic β-adrenergic receptor density and distribution (*10*) can now be imaged using PET. Several positron-emitting compounds have been developed to study presynaptic SNS function (*11–14*). Among these, ^{11}C-meta-hydroxyephedrine (mHED), a tracer for the norepinephrine transporter (NET) mechanism (*15*) that recycles NE released from the sympathetic nerve terminal, has been shown to have clinical applicability (*7–9*). Carbon-11-labeled mHED has a high affinity for the NET sites. NET and vesicular storage are similar to that of NE, and ^{11}C-mHED has the advantage of limited metabolism of the tracer (*16,17*). It has low nonspecific

Received Mar. 11, 1997; revision accepted Oct. 21, 1997.
For correspondence or reprints contact: James H. Caldwell, MD, Division of Cardiology (111C), Veterans Administration Medical Center, Seattle, WA 98108.